HiSST: International Conference on
High-Speed Vehicle Science Technology

26–29 November 2018, Moscow, Russia

Modelling of Heat Transfer in Rocket Combustion Chambers Using Eddy-Dissipation Combustion Model

Victor P. Zhukov[1]

Abstract

In the work an extension of the eddy-dissipation model (EDM) is developed in order to simulate turbulent combustion of hydrogen in undiluted oxygen in rocket combustion chambers. The modification of the eddy-dissipation model allows eliminating of main demerits of the original EDM model. This is achieved by introducing additional parameters into the model, which limit the reaction rate and depend on the local stoichiometry and temperature. The main such parameter is "Maximum flame temperature", which depends on local stoichiometry and takes into account the dissociation of combustion products. The extension of the EDM model is based on the framework provided by ANSYS CFX. The new turbulent combustion model is validated against experimental data from three different sub-scale rocket combustors. The validation of the model is carried out against data on pressure and wall heat flux, which are the main target of simulations of rocket combustion chambers. The simulation results show some benefits of the new combustion model; however, they also suffer from the deficiencies of the used eddy-viscosity turbulence model (SST).

Keywords: *turbulent combustion, liquid rocket engines, CFD simulations, non-premixed flames, hydrogen*

1. Introduction

Most of us associate rocket combustion chambers with high turbulence, pressures, and temperatures, which is true. At high pressures and temperatures, chemical reactions are so fast that allow to use the assumption of thin flame, i.e., of infinitely fast chemistry. This assumption holds very well for hydrogen in rocket combustion chambers [1]. The thin-flame assumption greatly simplifies the modeling of turbulent combustion as now there is no need to solve kinetic equations, since they are infinitely fast. However, this does not mean infinitely fast combustion. Now combustion rate is limited by other processes: turbulent mixing or fuel evaporation. In the most turbulent combustion models, which are used the thin-flame assumption, combustion rate is proportional to the rate of turbulent mixing. The most popular model of turbulent combustion in computational fluid dynamics simulations is the eddy-dissipation model [2]. The model is attractive not due to the accuracy but simplicity. The combustion is described as a single stage process. The present work deals with the case of the combustion of pure hydrogen and oxygen, so

$$\mathrm{H_2} + 0.5\,\mathrm{O_2} \longrightarrow \mathrm{H_2O}. \tag{1}$$

The reaction rate is given by the following expression

$$R = A\frac{\epsilon}{k}\min([\mathrm{H_2}], 2[\mathrm{O_2}]), \tag{2}$$

where A is a model constant, which usually equals to 4, ϵ and k are turbulent eddy dissipation and turbulent kinetic energy, respectively. The model is so crude that the authors of the EDM model tried to solve some of the problems of the model already in their original work [2]. They introduced a product limiter, which makes reaction rate dependent on the concentration of reaction products when

[1] *Institute of Space Propulsion, German Aerospace Center (DLR), Langer Grund, 74239 Hardthausen, Germany, victor.zhukov@dlr.de*

their concentration is small enough. However, this limiter is not used here. The EDM model has a clear physical interpretation: the reaction rate is proportional to the turbulent mixing timescale and to the average concentration of a deficient reactant. In contrast to other combustion models and other similar models like the eddy break-up model [3] and the eddy-dissipation-concept model [4], there is no complicated kinetic mechanism with intermediates in the model, and there is no splitting in different turbulent scales. There is only one global reaction step and one general turbulent timescale.

The main disadvantage of the EDM model in rocket combustion chamber is that it gives a very high flame temperature. Actually, the prediction of gas temperature is the main goal of Computational Fluid Dynamics (CFD) simulations of rocket combustion chambers. Nowadays, it is also possible using CFD simulations to predict the dynamics of combustion processes in rocket combustion chambers: engine firing and onset of combustion instability. However, the main thing, which is required from CFD simulations for the design of rocket combustion chambers, is an accurate prediction of thermal loads. The accurate predictions of heat fluxes requires the accurate simulation of temperature field in combustion chamber. Thus, the main requirements for combustion model is the accurate prediction of the temperature of burned gases. The direct use of Eq. (1) gives a flame temperature near 5000 K while the flame temperature in rocket combustion chambers amounts to around 3500 K. The temperature of H_2–O_2 flame is significantly lower than 5000 K due to the significant part of H_2O dissociates at temperatures above 3500 K. At $T=3600$ K and $p=60$ bar the equilibrium composition of water vapor in mole fractions is following (according to [5]):

x_{O_2}	x_O	x_{H_2}	x_{OH}	x_H	x_{H_2O}
0.035	0.015	0.116	0.095	0.033	0.706

The dissociation of water can be taken into account through a kinetic mechanism with several reactions and intermediates: OH, H, O_2, etc. However, the EDM model does not assume multi-step reaction or mechanism with many reactions. The direct use of the EDM model with a kinetic mechanism of many reactions results in a non-physical results because Eq. (2) results in a wrong balance between rates of different reactions and, consequently, in a wrong chemical equilibrium state. To overcome this and other demerits of the original EDM model, the following extension of the model is proposed.

2. Extension of the eddy-dissipation model

All simulating results presented in this work were obtained using the commercial computational fluid dynamics code ANSYS CFX [6]. The proposed extension of the EDM model is based on the framework provided by CFX for this model. CFX also allows users to define their own constants, expressions, functions, routines, etc. To solve the problem with too high flame temperature, CFX offers a simple solution that is to specify explicitly a maximum flame temperature. When the temperature of gas exceeds this parameter, the reaction rate is set to zero. However, this does not solve the problem completely. The temperature of burnt gases will exceed the adiabatic flame temperature in areas where the mixture equivalence ratio is not the same as the average equivalence ratio. To overcome this problem, it is necessary to set "Maximum flame temperature" dependent on mixture composition. In present case, a new parameter was defined which reflects a local equivalence ratio. This is the mass ratio of oxygen to hydrogen in mixture (or abbreviated MROH):

$$MROH = \left[Y_{O_2} + \frac{8}{9}Y_{H_2O} + 0.01\right] / \left[Y_{H_2} + \frac{1}{9}Y_{H_2O} + 0.01\right]. \quad (3)$$

The additional term "0.01" is needed to avoid the situation when $MROH$ is equal to zero or infinity. The adiabatic flame temperatures itself are calculated using CEA [7] or other similar code, see Table 1. (The focus of the present work is hydrogen rocket combustion chambers, which are usually cryogenic; thus, the initial temperature of the propellants amounts to 160 K in Table 1.) The effect of the variable "Maximum flame temperature" instead of a single value (e.g., 3660 K) is not large and was shown in work [8]. The difference between the single value and the variable "Maximum flame temperature" is visible only in very lean or reach mixtures.

In the EDM model the reaction rate does not depend on temperature. This causes two problems:

Table 1. Temperatures of H_2–O_2 flames at $T_{ini} = 160$ K and $p = 80$ bar [7]

$MROH$	0.84[a]	1	2	3	4	5	6	7	8	9	10	12	14	16	20	32	64	80	128	200	265[a]
T, K	0	1158	1963	2601	3072	3384	3568	3651	3665	3641	3598	3491	3380	3271	3065	2534	1669	1430	1026	750	0

[a] Explosion limits at 100 bar according to [9].

a combustion of propellants even at cryogenic temperatures and a sharp drop of the reaction rate behind the flame front when the gas temperature exceeds the "Maximum flame temperature". The first problem is solved by a "standard" approach: the introduction of an auxiliary parameter called "Extinction temperature". When the fuel mixture has a temperature below the "Extinction temperature", the reaction rate is set to zero. This parameter should reflect the flammability limits of H_2–O_2 mixture at low temperatures. There is no literature data on the flammability limits at cryogenic temperatures. However, an idea about the flammability limits can be got by modeling a laminar free premixed flame. In the present work, we used the kinetic model by Burke et al. [10], which is the closest to experimental data at the pressures above 10 atm, and the computer code PREMIX [11], which is the part of the software package CHEMKIN. As a result of the analysis of H_2–O_2 flames, the following expression has been used for the "Extinction temperature":

$$T_{ext} = 170\ [\mathrm{K}] \cdot ((\ln(MROH) - 1.7)^2 + 1). \tag{4}$$

This expression is not accurate and only a convenient function. In reality, the value of the "Extinction temperature" can be set by any other method or function.

The sharp drop of the reaction rate behind the flame front does not adversely affect the simulating results itself, but the presence of such singular points decreases the convergence of the solver. This problem was solved by setting model constant A dependent on temperature and the mass fraction of water vapor

$$A = 5 \cdot (1 - Y_{H_2O}^2) \cdot (\tanh((T - T_{ext})/100\ [\mathrm{K}]) + 1). \tag{5}$$

Now the reaction rate smoothly decreases at temperatures near T_{ext} and when the mass fraction of water (the product of the reaction) approaches 100%. This modification of the model results in a smoother spatial distribution of reaction rate across the chamber and allowed a tenfold decrease of mean residuals.

The present extended EDM model has two additional parameters for modeling the interaction between flame and turbulence. The turbulent mixing rate ϵ/k becomes large close to walls due to the drop of k. Therefore, the value of ϵ/k in Eq. (2) is limited to a value of $5 \cdot 10^3$ s^{-1}, which is set by a parameter called "Mixing Rate Limit" in CFX [12]; otherwise, the reaction rate goes up unnaturally near walls. At a certain level of turbulence, the dissipation of heat and radicals leads to flame quenching. In regions of high turbulence, when the turbulence time scale is smaller than a chemical time scale, local extinction occurs in the present model, i.e., the reaction rate is set to zero. The chemical time scale is defined in the present model as a ratio of laminar flame thickness δ to laminar flame velocity S_u. The flame thickness is evaluated using Blint's correlation [13]:

$$\delta = 2\delta_b = (\lambda/C_p)_b/(\rho_u S_u), \tag{6}$$

where indexes u and b denote unburnt and burnt states, respectively. The laminar flame velocity is calculated using the already mentioned mechanism of Burke et al. [10] and flame code PREMIX [11]. In our earlier works [8, 14], turbulence mixing time scale k/ϵ was used for the comparison with the chemical timescale; however, later the Kolmogorov time scale has been used instead of the mixing time scale ($\tau_{mix} = k/\epsilon$). This mechanism provides flame extinction near the injector tip. The weaker the flame near injector, the more oxygen crosses the flame. This slightly changes the distribution of oxygen over the cross-section of combustor. The present simulation results obtained using the Kolmogorov time scale are marginally better than the earlier results in [8, 14].

3. Numerical Modeling

It necessary to say a few words on numerical models and setups used here. As it was mentioned above, the modeling was done using ANSYS CFX [6]. The flow is modeled using the Favre averaged Navier–Stokes equations. Turbulence has been modeled using the SST $k-\omega$ turbulence model using the standard values of the coefficients and the "automatic" wall treatment [6]. The transport has been modeled with a turbulent Schmidt number of 0.7 (the value of 0.7 is recommended for high-Reynolds-number jet flows by Yimer et al. [15]). The turbulent Prandtl number was set to the default value in CFX which equals 0.9.

All components of the gas mixture (H_2, O_2, and H_2O) have significant distinctions from ideal gas under conditions typical for rocket engines; therefore, an accurate modeling of thermodynamic properties is required. Cryogenic O_2 and H_2 are modeled using the Peng–Robinson real gas equation of state. The enthalpy and the entropy of the individual components have been defined using NASA polynomials [16]. The dynamic viscosity and the thermal conductivity of H_2, O_2, and H_2O have been defined using the Sutherland's law with coefficients recommended by White [17]. The diffusion coefficients have estimated using the data from Kikoin [18]. The mixture molecular transport properties are calculated from the properties of the individual components using the equation by Mathur et al. for the thermal conductivity [19] and Wilke's formula for the viscosity [20], i.e., using the same equations as Chemkin [21]. The accuracy of both mixing rules (Mathur et al. and Wilke) in undiluted H_2–O_2 mixtures is discussed in [22].

4. Results

4.1. Penn State test case

A test case, which became the first well-known test case for the validation of CFD models for rocket combustion chambers, got the unofficial name "Penn State test case" (also known as RCM-1) [23]. This test case is a starting point for CFD modeling of rocket combustion chambers due to its relative simplicity. By this reason, this test case was modeled by many researchers [8, 24–28].Two works [24, 27] are collaborative works where authors compared different CFD approaches.

The configuration of the experimental setup corresponds to a staged combustion cycle operating with gaseous oxygen and hydrogen propellants [23]. The experimental setup consisted of two preburners and a main combustion chamber. The main combustion chamber has a single co-axial injector and is fueled by fuel-rich and oxygen-rich preburner gases. Within this test case, the results of wall heat flux measurements are supposed to be a target of simulations.

In Fig. 1, on can see a comparison of different CFD models with the experiment. The results obtained using the extended EDM model are named as CFX, DLR-LA (the used code, and the German abbreviated name of our institute). The selection of other simulations is determined by the similarity with our numerical model. All simulation results shown in Fig. 1 were obtained in quasi-two-dimensional axisymmetric domains by solving the Reynolds-averaged Navier–Stokes equations (RANS). The numerical setup used by us is described in the detail in earlier work [8]. The results presented here are slightly better than those presented earlier due to the use of the Kolmogorov time scale instead of the mixing time scale for the modelling of extinction at high turbulence.

Figure 2 shows simulated flow and temperature fields in the Penn State combustor. The simulation results look typical for RANS simulations. Many researchers were not very successful in modeling of heat transfer in this test case [24, 26, 28, 29]. The main critical point in this test case is the modeling of the recirculation zone in the corner between the sidewall and the front wall because the maximum of heat flux is located near the flow attachment point. If a model correctly predicts the size of the recirculation zone and the flame temperature then the simulation results automatically lie near the experimental points. That is why, the accuracy of the simulation results given by our model is not surprising because the SST turbulence model used here shows very good results in the prediction of the recirculation zone behind a backward facing step [30]. Indeed, simulation results in the Penn State test case are not

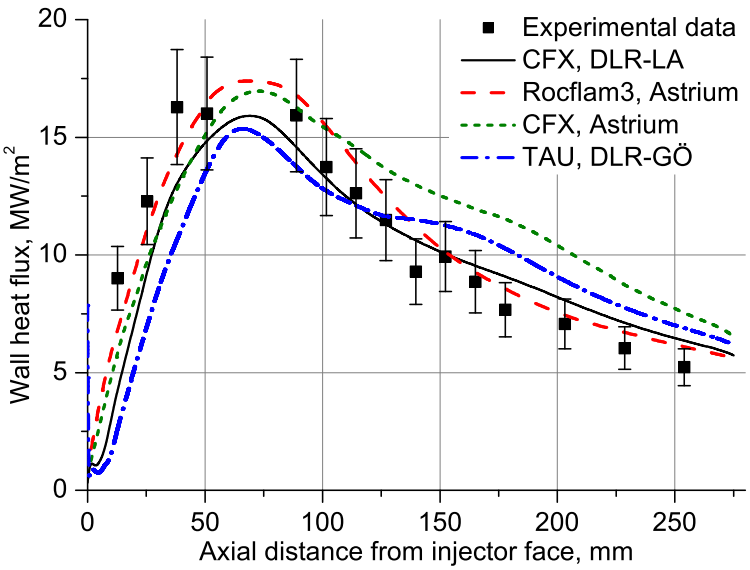

Fig 1. Comparison of the results of the extended EDM model (black line) with experimental data [23] and simulation results from other models [27]

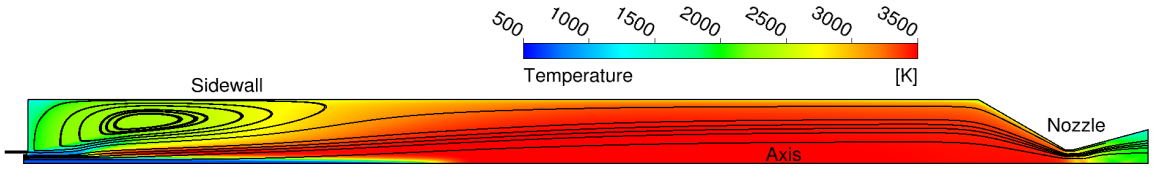

Fig 2. Simulated flow and temperature fields in the Penn State combustor

very sensitive to used combustion model. The simulations presented in Fig. 1 use different combustion models ("Rocflam3, Astrium" — equilibrium based PPDF, "CFX, Astrium" — flamelet, "TAU, DLR-GÖ" — finite rate chemistry without turbulence-chemistry interaction, and "CFX, DLR-LA" — the extended EDM model), but the results are close to each other. This is due to the fact that the Penn State combustor was fueled by hot partially burned gases, which immediately react with each other, so the duty of the combustion model is only to predict accurately the temperature of burnt gases.

4.2. Combustion chamber with porous injector

The second test case is much more complex than the Penn State test case. The details of this case are published in [14, 31]. The test case has a feature which is a porous injector head. In this test case, liquid oxygen (LOx) is fed through many distributed single injectors while cold hydrogen (100 K) is fed into a combustion chamber through a porous plate. This injector is a new concept under development at the Institute of Space Propulsion. The concept has some advantages over coaxial injectors, which are conventional for rocketry. According to the hot-tests at the Institute of Space Propulsion of the German Aerospace Center (DLR-Lampoldshausen) [32], the porous injector head (Fig. 3) allows to maintain the high combustion efficiency over the wide throttling range from 40% to 130%. Besides the low manufacture cost and the throttling capability, porous injector head has two additional advantages over conventional coaxial injectors. Porous injector head operates at a smaller pressure drop than injector heads with coaxial injectors. Secondly, the small diameter of the injectors in a porous head results in a small jet break-up distance which allows reducing combustor length.

The numerical setup used in this test case is described in details in the original works by Zhukov and Suslov [14, 31]. Liquid oxygen was treated in the simulations as a real gas which obeys the Peng–Robinson

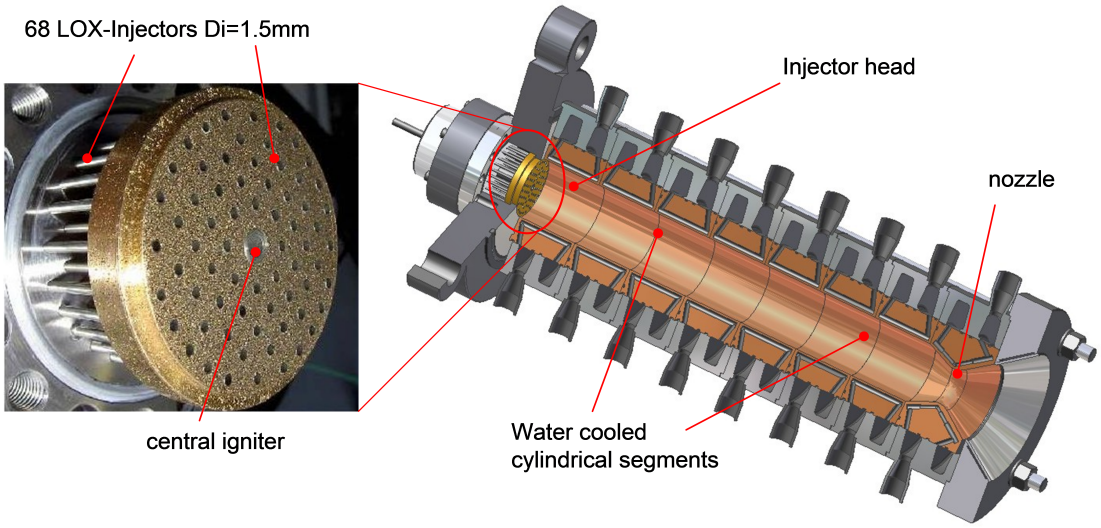

Fig 3. The photo of porous injector head API-68 and the cross-section of sub-scale combustion chamber model "B" [14]

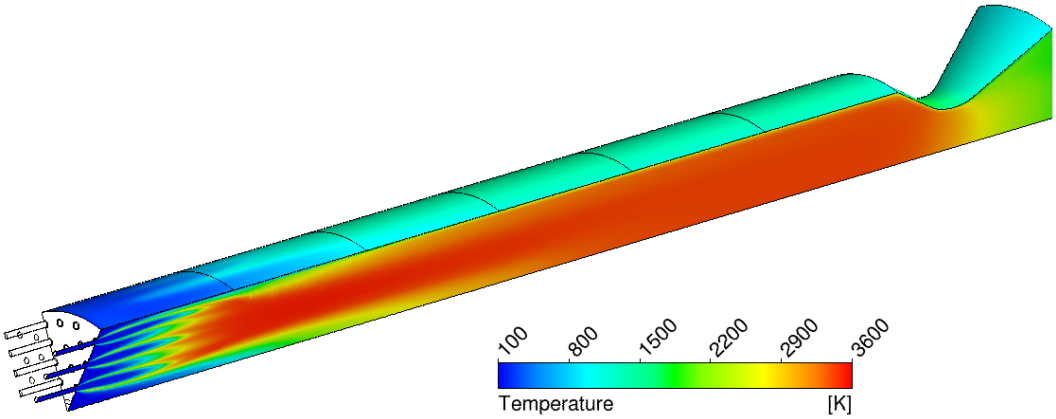

Fig 4. Temperature fields simulated by the extended EDM model at the symmetry plane and at the walls of the combustion chamber.

equation of state. In earlier work [33], Zhukov and Suslov showed that simulations of the combustion chamber with the porous injector head should be carried out in a three-dimensional (3D) formulation. In order to have a correct representation of the arrangement of oxygen injectors, the simulations were carried out in the eighth part of the combustion chamber, see Fig. 4. As one can see in the figure, the outer injectors have different contributions to the wall head flux.

The transition from 2D to 3D problem formulation significantly increases the computational cost. Certainly, using a heavy combustion model with many transport and differential equations would make it impossible to simulate the combustion chamber in 3D geometry using a single workstation, in this case Dell T7500 with two Intel Xeon E5645 processors. Other options for such computational resources can be the use of the flamelet approach or the equilibrium chemistry model [27]. Both these combustion models also use the thin-flame assumption; however, they both also assume unlimited mixing rate or infinitely fast chemistry at "mesoscopic" level. Moreover, the adiabatic flamelet model assume no further reaction behind the flame front. In work [14], we carried out the comprehensive comparison between the extended EDM model and the flamelet approach, in this case the Extended Coherent Flame Model (ECFM) [34], which includes also turbulence-chemistry interaction. The comparison (Fig. 5) showed

that the ECFM model predicts pressure in the combustion chamber lower by 1–1.5 bar while the prediction of the EDM model is within the error margins. The difference between the models considered in detail in [14]. The low pressure in the combustion chamber with the ECFM model is explained by the absence of chemical reactions in burnt gases, namely in the nozzle. From the equations given in Rocket Propulsion [35], it is possible to connect combustion chamber pressure p_c with the speed of sound c_{th} and temperature T_{th} in the throat

$$p_c = \frac{\dot{m}}{A_{th}} \frac{c_{th}}{\gamma \left(2/(\gamma+1)\right)^{\frac{\gamma}{\gamma-1}}} \approx \frac{\dot{m}}{A_{th}} \frac{c_{th}}{0.68} \tag{7}$$

$$\gamma = C_p/C_V \approx 1.2 \text{ [5]}, \; c_{th} = \sqrt{\frac{\gamma}{\mu} R T_{th}}, \tag{8}$$

where $\dot{m}$ is the total propellant mass flow rate; A_{th} is the throat area, and μ is molar mass. The extended EDM model predicts higher temperature in the throat, because the mixture retains the reactivity in the nozzle since the temperature there is below the "Maximum flame temperature". Whereas the flamelet combustion model means a chemically frozen flow in the nozzle. The lower temperature in the nozzle given by the ECFM model also results in the too low wall heat flux in the nozzle [14] while the results of the extended EDM model agree with the experimental data, see Fig. 6.

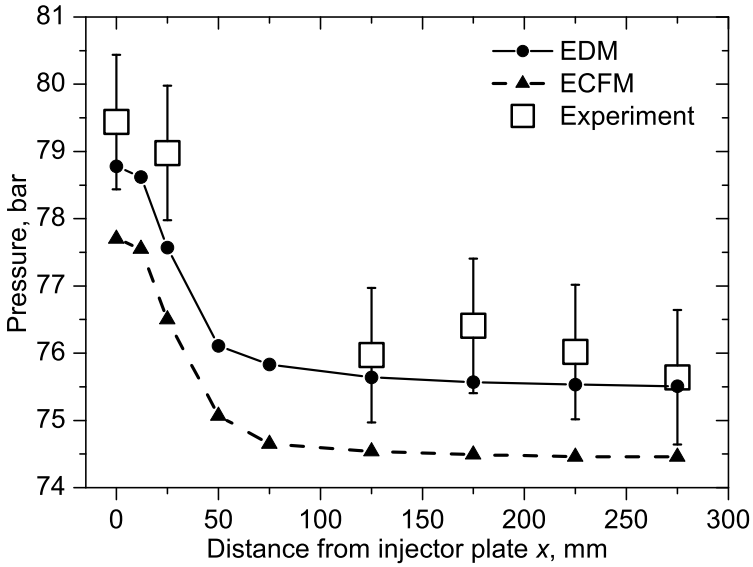

Fig 5. Pressure profile in the combustion chamber: experimental data and simulation results

The model was also validated at different oxidizer-to-fuel ratios (ROF) [31]. The results are presented in Fig. 6. The difference between simulation and experiment exceeds the experimental error, which is not less than ± 3 MW/m^2, but is still in an acceptable range. The accuracy of wall heat flux predictions depends not only on the accuracy of combustion model but also on the accuracy of the boundary layer modeling which is very difficult in this particular case where flames of some injectors penetrate into the boundary layer.

4.3. Single coaxial injector combustion chamber

The third test case simulated here was obtained at test facility P8 at the German Aerospace Center (DLR-Lampoldshausen). The test case was presented on conferences in 2015 and 2016 [36, 37], and it was already simulated in [38, 39]. Although the combustion chamber has only one coaxial injector, this test case is not easier for CFD modeling than the previous one. Now both propellants are injected at cryogenic temperatures, and a significant part of the fuel is used for a film cooling and injected at a very high speed.

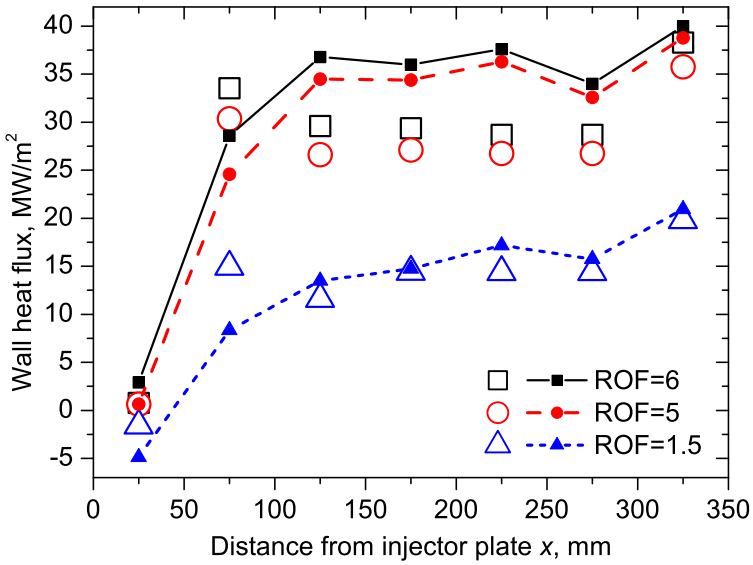

Fig 6. Comparison of the measured and predicted wall heat fluxes. Open symbols — experiment; lines and solid symbols — simulations

The used combustion chamber was specifically developed and manufactured for intra-chamber studies of injection and combustion by providing optical access for the application of optical diagnostics. A sketch of the chamber is shown in Fig. 7. The combustion chamber is segmented into four interchangeable water-cooled sections and a nozzle. Thus, the instrumented section can be placed at various axial locations. This feature has been used to achieve optical access along the full combustion chamber length from $x = 0$ mm to $x = 370$ mm. This distance is the same as the length of real rocket engines up to nozzle throat. The inner diameter of the presented sub-scale combustion chamber is 50 mm. The detailed descriptions of the combustion chamber can be found in original works [36, 37, 40].

The hot-fire tests were carried out at pressures of 40, 50, and 60 bar for three different ratios of oxidizer-to-fuel at the injector (ROF_{inj}): 4, 5, and 6. Rearranging the sections of the combustion chamber, pressure and temperature measurements were obtained at different locations along the chamber axis. In order to carry out the measurements over the whole length of the chamber for the nine different load points, the hot-fire tests were repeated a considerable number of times. The reproducibility of the test parameters for different chamber configurations amounts to $\pm$2%.

The simulations have been performed in a 2D axisymmetric domain using the same numerical setup as before; however, all components (O_2, H_2, H_2O, and N_2(~1%)) are modelled using the Peng–Robinson real gas equation of state. The only one load points, which has supercritical pressure and $ROF_{inj} = 6$, has been simulated. The simulations results are preseted in Figs. 8 and 9.

The model shows a good agreement with the experimental data [36]. The simulation is complicated by the presence of a massive film cooling and by an uncertainty in the wall heat flux, which was not measured in the experiment. The cooling film injected at the high speed and the flame of the coaxial injector generate an unstable system of vortices between theses two flows near the front wall. Small changes in the flame or in the film result in a significant change of the arrangement of the vortices, and this significantly slows down the solver convergence. Nevertheless, the numerical model delivers the good results.

5. Discussion

The extended EDM model was successfully validated against the experimental data from the three different rocket combustors. The simulation results show no problems or nonphysical behavior associated

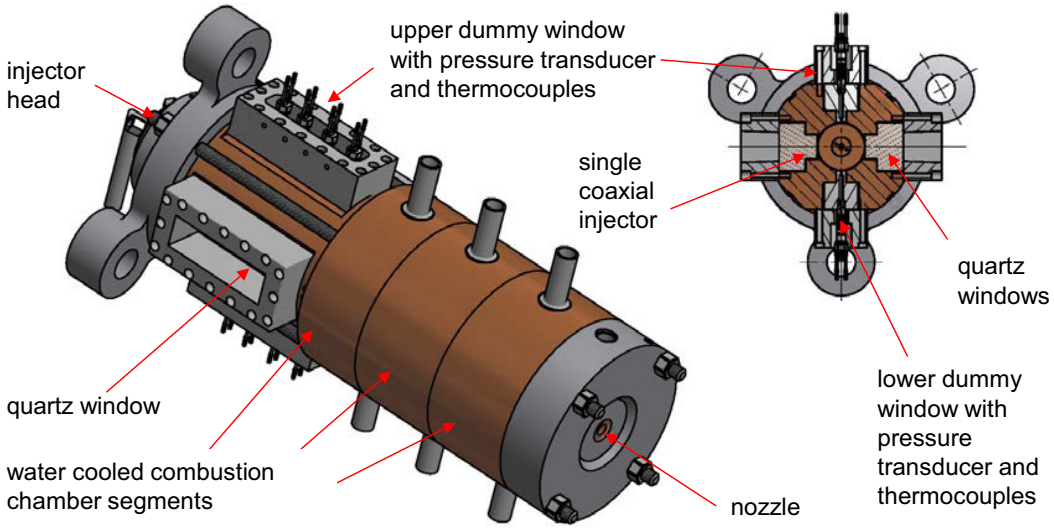

Fig 7. DLR subscale combustion chamber model "C" [36]

with the low injection temperature of hydrogen. In other words, the model shows the good performance at the different injection conditions. Thus, the developed model can operate in the wide ranges of fuel-to-oxidizer ratios and of injection temperatures starting from cryogenic. Another advantage of the new model is that it can be easily adapted for methane, which is considered as a future rocket fuel by ESA, SpaceX, Blue Origin, and Roskosmos.

The new model was compared with the flamelet based model, but there is also a need for comparison with the equilibrium chemistry model [41]. It also utilizes single-step global reaction scheme, but the reaction rate is not limited and equals to infinity. Using the equilibrium chemistry model model, Preclik et al. simulated full-scale rocket engines and obtained a good agreement with experimental data on wall heat fluxes in sub-scale rocket combustors [41]. However, the assumption about the infinite reaction rate may lead some problems. This assumption is very strong. It is certainly not valid close to walls, in regions with low temperatures or where the mixture is very lean or rich, and it is not valid for hydrocarbons.

The EDM model can be adapted for the use with scale-resolved turbulence models: SAS, DES, and LES. In this case, the simulated structures will transport reactants towards the flame front while the modeled structures will be responsible for the limiting mixing within the flame front. The mixing rate can be defined in the same way as it is defined in ANSYS in the the realization of the EDM model for LES [42]:

$$\tau^{-1} = \sqrt{2 S_{ij} S_{ij}}, \; S_{ij} = \frac{1}{2}\left(\frac{\partial u_i}{\partial x_j} + \frac{u_j}{\partial x_i}\right). \tag{9}$$

The extended EDM model has shortcomings as well. First, it inherits all weaknesses of the thin-flame assumption and depends on the validity of this assumption. The validity of the model is questionable outside rocket engine conditions, which mean a non-premixed combustion of high energetic propellants at high pressures and temperatures. The model considers the combustion of propellants as a single-stage process without the formation of intermediates. There is no self acceleration of reaction due to the formation of radicals in the model. In the absence of OH and CH in the model, the comparison of simulation results with experimental data on flame chemiluminescence requires additional modelling.

Temperature makes the most impact on the reaction rate; however, the reaction rate (Eq. 2) in the EDM moel, as in many other turbulent combustion models, does not depend on temperature. The reaction

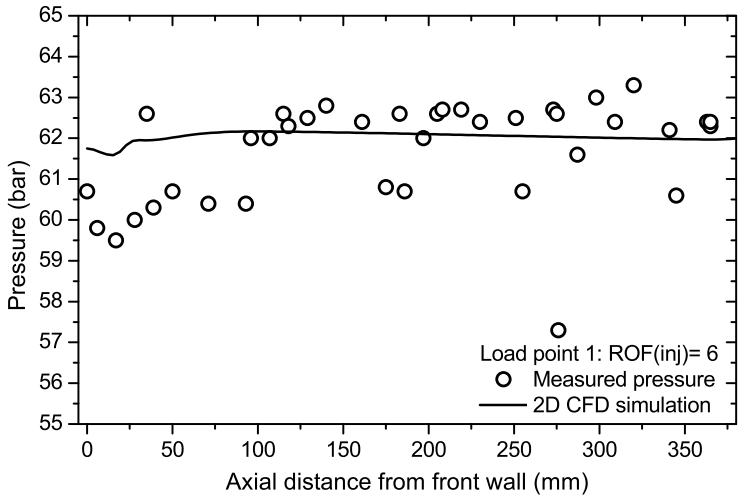

Fig 8. Static wall pressure profile at at Load point 1: ROF$_{inj}$ = 6, 60 bar

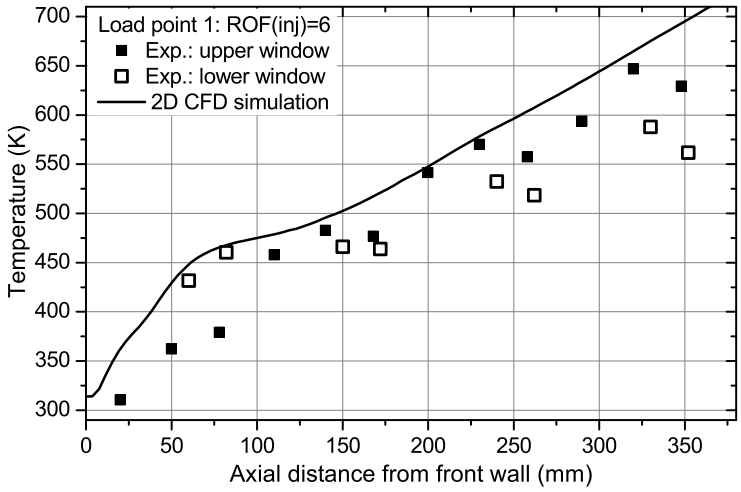

Fig 9. Wall temperature at Load point 1: ROF$_{inj}$ = 6, 60 bar

rate should be low at low temperatures and high at high temperatures; close to the chemical equilibrium state, the reaction should slow down. The proposed extension of the EDM model partially resolves this problem; however, it cannot offer the same accuracy as a kinetic model with many reactions.

6. Conclusions

The extension of the EDM model has been developed for the application in hydrogen rocket combustors. The extension resolves the major shortcomings of the EDM model. The extended EDM model was validated against experimental data on wall heat fluxes and pressures in the three different combustion chambers in the wide ranges of oxidizer to fuel ratios and of injection temperatures.

The provided coefficients and data allow to use the extended EDM model for modeling hydrogen rocket combustors at pressures about 80 bar directly or after corresponding correction of the "Maximum flame temperature" at any other pressures. The given approximations for "Extinction temperature" T_{ext} and for model constant A are "convenient" functions; thus, they can be defined by other ways. The chemical time scale can be defined by an alternative way too.

The advantages and disadvantages of the new model in comparison to other models are described in the present paper. The proposed methodology also allows extending the EDM model for methane. In the paper, it is shown how the new model can be also used with scale-resolved turbulence models: SAS, DES, and LES.

References

1. Ivancic, B., Mayer, W.: Time- and length scales of combustion in liquid rocket thrust chambers. J. Propul. Power 18(2), 247–253 (2002). doi: 10.2514/2.5963
2. Magnussen, B.F., Hjertager, B.H.: On mathematical models of turbulent combustion with special emphasis on soot formation and combustion. In: Symposium (International) on Combustion, vol. 16, pp. 719–729 (1977). doi: 10.1016/S0082-0784(77)80366-4
3. Spalding, D.: Mixing and chemical reaction in steady confined turbulent flames. In: Symposium (International) on Combustion, vol. 13, pp. 649–657 (1971). doi: 10.1016/S0082-0784(71)80067-X
4. Magnussen, B.F.: On the structure of turbulence and a generalized eddy dissipation concept for chemical reaction in turbulent flow. In: 19th Aerospace Sciences Meeting (1981). doi: 10.2514/6.1981-42
5. Vargaftik, N.: Tables on the thermophysical properties of liquids and gases: in normal and dissociated states. Hemisphere Publishing Corporation (1975)
6. ANSYS, Inc., Canonsburg, PA, USA: ANSYS CFX-Solver Theory Guide (2012). Release 14.5
7. McBride, B.J., Gordon, S.: Computer program for calculation of complex equilibrium compositions and applications. Tech. Rep. 1311, NASA (1996)
8. Zhukov, V.P.: Computational fluid dynamics simulations of a GO_2/GH_2 single element combustor. J. Propul. Power 31(6), 1707–1714 (2015). doi: 10.2514/1.B35654
9. Schröder, V., Holtappels, K.: Explosion characteristics of hydrogen-air and hydrogen-oxygen mixtures at elevated pressures. In: International Conference on hydrogen safety, Congress Palace, Pisa, Italy (2005)
10. Burke, M.P., Chaos, M., Ju, Y., Dryer, F.L., Klippenstein, S.J.: Comprehensive H_2/O_2 kinetic model for high-pressure combustion. Int. J. Chem. Kinet. 44(7), 444–474 (2012). doi: 10.1002/kin.20603
11. Kee, R.J., Grcar, J.F., Smooke, M.D., Miller, J.A.: A Fortran program for modeling steady laminar one-dimensional premixed flames. Tech. Rep. SAND85-8240, Sandia National Laboratories, Livermore, USA (1985)
12. ANSYS, Inc., Canonsburg, PA, USA: ANSYS CFX-Solver Modeling Guide (2012). Release 14.5
13. Blint, R.J.: The relationship of the laminar flame width to flame speed. Combust. Sci. Technol. 49(1-2), 79–92 (1986). doi: 10.1080/00102208608923903
14. Zhukov, V.P., Suslov, D.I.: Measurements and modelling of wall heat fluxes in rocket combustion chamber with porous injector head. Aerosp. Sci. Technol. 48, 67–74 (2016). doi: 10.1016/j.ast.2015.10.021
15. Yimer, I., Campbell, I., Jiang, L.Y.: Estimation of the turbulent schmidt number from experimental profiles of axial velocity and concentration for high-Reynolds-number jet flows. Can. Aeronaut. Space J. 48(3), 195–200 (2002). doi: 10.5589/q02-024
16. Burcat, A.: Third millennium ideal gas and condensed phase thermochemical database for combustion. Tech. Rep. 867, Technion Aerospace Engineering, Haifa, Israel (2001)

17. White, F.M.: Viscous Fluid Flow, 2 edn., chap. Preliminary Concepts, pp. 29,32. McGraw–Hill, New York (1991)

18. Kikoin, I.K. (ed.): Tables of physical values. Atomizdat, Moscow (1976)

19. Mathur, S., Tondon, P.K., Saxena, S.C.: Heat conductivity in ternary gas mixtures. Mol. Phys. 12(6), 569–579 (1967)

20. Wilke, C.R.: A viscosity equation for gas mixtures. J. Chem. Phys. 18(4), 517–519 (1950). doi: 10.1063/1.1747673

21. Kee, R.J., Dixon-Lewis, G., Warnatz, J., Coltrin, M.E., Miller, J.A.: A FORTRAN computer code package for the evaluation of gas-phase, multicomponent transport properties. Tech. Rep. SAND86-8246B, Sandia National Laboratories (1986)

22. Zhukov, V.P., Pätz, M.: On thermal conductivity of gas mixtures containing hydrogen. Heat Mass Transfer 53(6), 2219–2222 (2017). doi: 10.1007/s00231-016-1952-9

23. Pal, S., Marshall, W., Woodward, R., Santoro, R.J.: Wall heat flux measurements for a uni-element GO_2/GH_2 shear coaxial injector. In: 3-rd International Workshop "Rocket Combustion Modeling". Snecma, Safran Group, Vernon, France (2006)

24. Tucker, P., Menon, S., Oefelein, J., Yang, V., Merkle, C.: Validation of high-fidelity CFD simulations for rocket injector design. In: 44th AIAA/ASME/SAE/ASEE Joint Propulsion Conference and Exhibit (2008). doi: 10.2514/6.2008-5226. AIAA 2008-5226

25. Sozer, E., Vaidyanathan, A., Segal, C., Shyy, W.: Computational assessment of gaseous reacting flows in single element injector. In: 47th AIAA Aerospace Sciences Meeting including The New Horizons Forum and Aerospace Exposition (2009). doi: 10.2514/6.2009-449. AIAA 2009-449

26. Lian, C., Merkle, C.L.: Contrast between steady and time-averaged unsteady combustion simulations. Comput. Fluids 44(1), 328–338 (2011). doi: 10.1016/j.compfluid.2011.01.032

27. Ivancic, B., Riedmann, H., Frey, M., Knab, O., Karl, S., Hannemann, K.: Investigation of different modeling approaches for CFD simulation of high pressure rocket combustors. In: 5th European Conference for Aeronautics and Space Sciences (EUCASS) (2013). Paper id: 94

28. Lempke, M., Keller, R., Gerlinger, P.: Influence of spatial discretization and unsteadiness on the simulation of rocket combustors. Int. J. Numer. Meth. Fluids 79(9), 437–455 (2015). doi: 10.1002/fld.4059

29. Karl, S., Hannemann, K.: Application of the DLR TAU-code to the RCM-1 test case: Penn state preburner combustor. In: 3-rd International Workshop "Rocket Combustion Modeling". Snecma, Safran Group, Vernon, France (2006)

30. ul Haque, A., Ahmad, F., Yamada, S., Chaudhry, S.R.: Assessment of turbulence models for turbulent flow over backward facing step. In: Proceedings of the World Congress on Engineering, vol. 2, pp. 2–7 (2007)

31. Zhukov, V.P., Suslov, D.I.: Wall heat fluxes at different oxidizer to fuel ratios in rocket combustion chamber with porous injector head. In: 6th European Conference for Aeronautics and Space Sciences (EUCASS) (2015). Paper id: 177

32. Deeken, J., Suslov, D., Haidn, O., Schlechtriem, S.: Combustion efficiency of a porous injector during throttling of a LOx/H_2 combustion chamber. In: L. DeLuca, C. Bonnal, O. Haidn, S. Frolov (eds.) Progress in Propulsion Physics, vol. 2, pp. 251–264. EDP Sciences (2011). doi: 10.1051/eucass/201102251

33. Zhukov, V.P., Suslov, D.I., Haidn, O.J.: CFD simulation of flow in combustion chamber with porous injector head and transpirationally cooled walls. In: 4th European Conference for Aeronautics and Space Sciences (EUCASS) (2011). Paper id: 29

34. Colin, O., Benkenida, A.: The 3-zones extended coherent flame model (ECFM3Z) for computing premixed/diffusion combustion. Oil Gas Sci. Technol. 59(6), 593–609 (2004). doi: 10.2516/ogst:2004043

35. Barrère, M., Jaumotte, A., de Veubeke, B.F., Vandenkerckhove, J.: Rocket propulsion, chap. 2. Nozzle theory and characteristic parameters, pp. 59–129. Elsevier Pub. Co. (1960)

36. Suslov, D.I., Hardi, J., Knapp, B., Oschwald, M.: Hot-fire testing of LOX/H2 single coaxial injector at high pressure conditions with optical diagnostics. In: 6th European Conference for Aeronautics and Space Sciences (EUCASS) (2015)

37. Suslov, D.I., Hardi, J., Knapp, B., Oschwald, M.: Optical investigation of the LOX-jet disintegration processes at high pressure conditions in a LOX/H2 single coaxial injector combustion chamber. In: Space Propulsion 2016 (2016). Paper id: SP2016_3124815

38. Seidl, M.J., Aigner, M., Keller, R., Gerlinger, P.: CFD simulations of turbulent nonreacting and reacting flows for rocket engine applications. J. Supercrit. Fluids 121, 63–77 (2017). doi: 10.1016/j.supflu.2016.10.017

39. Fechter, S., Karl, S., Hannemann, V., Hannemann, K.: Simulation of LOx/GH2 single coaxial injector at high pressure conditions. In: 53rd AIAA/SAE/ASEE Joint Propulsion Conference (2017). doi: 10.2514/6.2017-4765. AIAA 2017-4765

40. Mayer, W.O.H., Ivancic, B., Schik, A., Hornung, U.: Propellant atomization and ignition phenomena in liquid oxygen/gaseous hydrogen rocket combustors. J. Propul. Power 17(4), 794–799 (2001). doi: 10.2514/2.5835

41. Preclik, D., Knab, O., Görgen, J., Hagemann, G.: Ch. 15: Simulation and analysis of thrust chamber flowfields: Cryogenic propellant rockets. In: M. Popp, J. Hulka, V. Yang, M. Habiballah (eds.) Liquid Rocket Thrust Chambers, pp. 527–551. AIAA (2004). doi: 10.2514/5.9781600866760.0527.0551

42. ANSYS, Inc.: ANSYS Fluent 12.0. Theory Guide (2009)